



Progress Highlight

A novel generic platform for chemical patterning of surfaces

Jost W. Lussi ^{a,c}, Roger Michel ^{b,1}, Ilya Reviakine ^{b,2},
Didier Falconnet ^b, Andreas Goessl ^{a,3}, Gabor Csucs ^c,
Jeffrey A. Hubbell ^{a,4}, Marcus Textor ^{b,*}

^a Department of Materials, Institute for Biomedical Engineering,
Swiss Federal Institute of Technology (ETH), Zurich, Switzerland

^b Department of Materials, Laboratory for Surface Science and Technology, BioInterfaceGroup,
Swiss Federal Institute of Technology (ETH), Zurich, Wolfgang-Pauli-Strasse 10,
ETH Hönggerberg, HCI H 525, CH-8093 Zurich, Switzerland

^c Department of Mechanical Engineering and Process Technology, BioMicroMetrics Group,
Swiss Federal Institute of Technology (ETH), Zurich, Switzerland

Abstract

Advancement in various fields ranging from biomaterials to cell biology is fostered by the evolution in patterning technology, that delivers smaller and smaller features exhibiting distinct (bio)chemical contrast and addressability. We have recently introduced a simple and versatile patterning technique based on selective adsorption from aqueous media of multi-functional organic molecules onto oxide substrates pre-patterned by lithographic methods. Here we demonstrate the use of this technique, termed selective molecular assembly patterning, for the preparation of cell-adhesive patterns of arbitrary geometry, and their use

* Corresponding author. Fax: +41 1 633 10 27.

E-mail address: marcus.textor@mat.ethz.ch (M. Textor).

¹ Current address: Department of Chemical Engineering, University of Washington, Seattle, Washington, USA.

² Current address: Department of Chemical Engineering, University of Houston, Houston, Texas, USA.

³ Current address: Baxter Bioscience, Vienna, Austria.

⁴ Current address: Institute for Biological and Chemical Engineering, Swiss Federal Institute of Technology Lausanne (EPFL), Ecublens, Switzerland.

to investigate the relationship between pattern geometry and the organization of elements of the cell adhesion apparatus, namely focal contacts and stress fibres. Cell-culture compatible substrates with patterns consisting of ligands for cell-adhesion or other receptors represent a promising experimental tool for investigating cell–surface interactions with the goal of elucidating the mechanisms of how cells sense structural cues of the extracellular matrix.

© 2004 Elsevier Ltd. All rights reserved.

Keywords: Surface patterning; Lithography; Self-assembly; Selective adsorption; Cell adhesion; Cell–surface interactions; Focal contacts; Stress fibers; Biochip; Cellomics

Contents

1. Main text	56
2. Experimental	64
2.1. Substrate preparation	64
2.2. Pre-patterning: creating material contrast	64
2.3. Surface modification: creating adhesion contrast	65
2.4. Surface characterisation	65
2.4.1. Fluorescence microscopy (FM)	66
2.4.2. Time-of-flight secondary ion mass spectrometry (ToF-SIMS)	66
2.4.3. Atomic force microscopy (AFM)	66
2.4.4. Cell experiments	66
Acknowledgments	67
References	67

1. Main text

A number of methods in biosensing and high-throughput screening rely on spatially addressable deposition and manipulation of biological moieties with high spatial fidelity. Since miniaturization and parallelization offer considerable practical and technical advantages, increasingly smaller structures with controllable biochemical properties are sought, such as micro- and nanoarrays of proteins and oligonucleotides [1–4]. In studies of cell biology and implant-host response, a detailed understanding of how surface structures of biomaterials translate into specific cellular responses [5–8] is another important area of investigation that benefits from well-defined patterns containing biological functionality at length scales comparable to those of substructures present on the surfaces of cells, i.e., the micrometer and sub-micrometer range.

Existing patterning techniques are not always able to address the requirements of the biosensor, cell biology, and biomaterials fields in an efficient manner. Surface

scratching, micromachining, blasting, and etching [9–11]—techniques with which the effects of surface topography on cell behaviour were initially studied—do not offer sufficient flexibility in terms of defining pattern geometries or surface chemistries. Soft lithography, which is arguably the most versatile collection of patterning tools available to date [12,13], allows a wide variety of μm -sized patterns to be created rapidly and efficiently and has been widely used in studies of cell behaviour on patterned surfaces [7,13–20]. Because it involves elastomeric (typically PDMS) stamps, however, there are limitations in terms of the type of pattern geometries (patch form, size and pitch combinations) that can be produced with sufficient fidelity. Furthermore, the fabrication of large surface areas, e.g., whole 4" wafers or large numbers of samples with constant pattern quality is currently not state-of-the-art. Contamination of the resulting surface with traces of the elastomer is also of some concern when applying soft lithography methods based on silicone materials [21]. Implementation of this method in an industrial setting and for a wider range of applications is thus difficult to envisage at this point.

To address the current limitations in biomolecular patterning, a novel patterning technology—selective molecular assembly patterning (SMAP)—has been developed. The basic feasibility of the SMAP process has been previously shown [22] for the case of simple square patterns that could as well be produced with existing patterning tools. Here we demonstrate for the first time that using SMAP, protein patterns of arbitrary geometry can be created in a reliable and reproducible manner over a wide range of length scales and used to study cell–surface interactions.

SMAP was designed and developed with potential industrial applications in mind. It holds the attractive simplicity associated with aqueous dip-and-rinse processes and is compatible with, but not dependent on, standard lithographic techniques, therefore being readily transferable to large scale production of patterned surfaces in the biosensor, high-throughput screening, and implant fields.

A schematic illustration of SMAP is presented in Fig. 1. First, a substrate (e.g. glass or silicon wafer) is prepared by coating it with thin layers of oxide, in this particular case with 50 nm TiO_2 and subsequently 12 nm SiO_2 (Fig. 1a). In the second step, material contrast, i.e., a surface presenting materials with different physical and chemical properties arranged in the desired geometrical pattern, is created using lithographic and etching techniques [12] (Fig. 1b). Samples exhibiting material contrast were routinely examined by atomic force microscopy (AFM) to follow the etching process and to ascertain the depth and the overall quality of the patterns. An AFM image of one of the patterns used in this study reveals the pattern of 21 nm deep, 15 μm long, and 1 μm wide grooves arranged in a Swiss cross-like structure around a central square region of the same depth (Fig. 2a). Time-of-flight secondary ion mass spectrometry (ToF-SIMS) confirms that the surface of the grooves and of the centre square is composed of titanium species (Fig. 2b). These were identified as TiO_2 by X-ray photoelectron spectroscopy (XPS, not shown) on identically treated samples with larger pattern structures. The presence of silicon oxide in the areas around the patterns and the absence of residuals of the resist used during the photolithographic process were confirmed by ToF-SIMS and XPS (not shown; see Section 2).

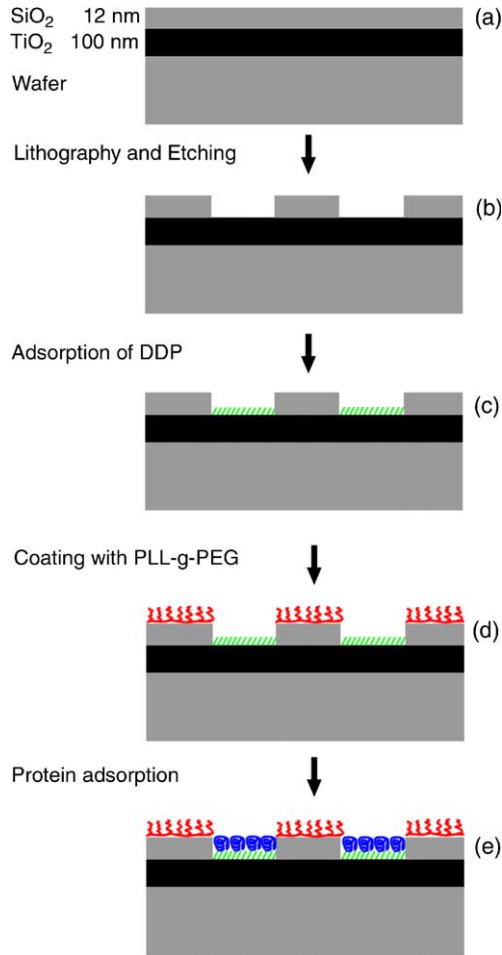


Fig. 1. Schematic illustration of the SMAP method. Material contrast created in oxides by lithographic techniques is converted, in a series of dip-and-rinse processes performed in aqueous solutions, into a contrast with respect to protein adsorption: (a) a polished silicon or transparent glass wafer is coated first with a 50 nm titanium oxide intermediate layer and then with a 12 nm thin silicon oxide top layer. (b) The desired patterns are created in the metal oxide layer by a combination of lithographic and etching processes. An inverted topology (with the titanium oxide layer on top of a silicon oxide film) has also been explored (not shown). (c) Adsorption of dodecyl phosphate (DDP) from aqueous solution leads to the formation of an oriented self-assembled monolayer on TiO_2 , making it hydrophobic. There is no interaction between DDP and the SiO_2 surface, which is left completely bare. (d) After rinsing with water, PLL-g-PEG adsorbs from a buffered solution to the bare SiO_2 , and to a lesser extent also to the DDP (not shown). After rinsing, the PLL-g-PEG-coated SiO_2 regions repel proteins completely, while the PLL-g-PEG adsorbed on the DDP is weakly bound and is exchanged with the adsorbing protein(s). (e) The chemical contrast between hydrophobic and protein-resistant areas can then be converted into an adhesive/biofunctional contrast by simply exposing the surface to proteins. Cell culture experiments were performed by using a serum-containing cell culture media. Solutions of individual proteins can also be used if purity is required, e.g., for protein assays.

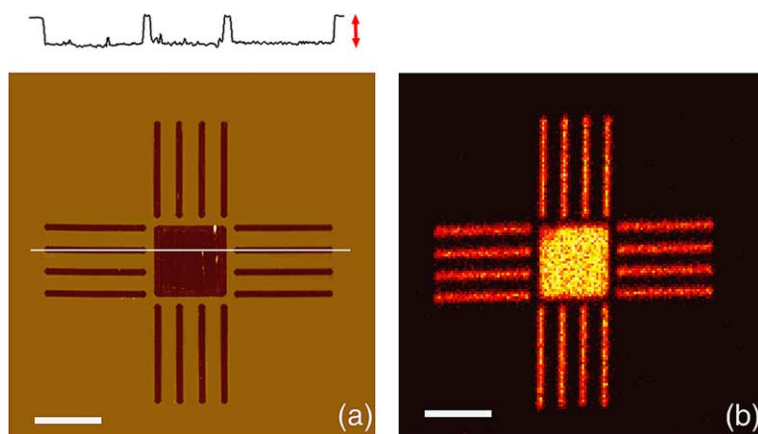


Fig. 2. Characterisation of the patterns prepared by the SMAP method. Patterns prepared by the SMAP method were characterised by surface sensitive techniques at various stages during their preparation. As an example, AFM (a) and ToF-SIMS (b–e) images characterising one of the two patterns used in this study from the pre-patterning stage to the development of adhesion contrast are shown (see Fig. 1b–e for the description of each of the stages). (a) An AFM image of the pre-patterned surface exhibiting material contrast (after the photolithography and etching steps, Fig. 1b). A Swiss cross-like pattern consisting of grooves arranged around a square, all ~ 15 – 21 nm deep (red double-headed arrow in the inset) is visible. The image was low-pass filtered. White line across the pattern indicates the location where the section shown in the inset was taken. Scale bar: $10\ \mu\text{m}$. (b) A ToF-SIMS image of the pre-patterned surface exhibiting material contrast (identical to the one AFM image shown in (a)). Higher brightness corresponds to higher counts of the Ti^+ ($m/z = 48$) secondary ions, which are seen to be restricted to the grooves and the central square. Approximately 100 counts per spot (256×256 data points per $150 \times 150\ \mu\text{m}^2$) were recorded for the Ti^+ -ions. Scale bar: $10\ \mu\text{m}$. (c) A ToF-SIMS image of the sample after self-assembly of DDP on the TiO_2 patches (Fig. 1c). Brighter areas correspond to higher counts of the sum of phosphate-specific PO_2^- ($m/z = 63$) and PO_3^- ($m/z = 79$) fragments [24]. Phosphates are seen to co-localise with the Ti species observed in (b) to the grooves and the central square. Despite the fact that the lateral size of the grooves is at the limit of the resolution of the technique, there is a clear difference in intensity with respect to the surrounding area. This is due to the high selectivity of the adsorption and self-assembly process of the DDP. Maximum counts (177) were recorded for the PO_2^- species. Scale bar: $10\ \mu\text{m}$. (d) A ToF-SIMS image of the sample after adsorption of PLL-g-PEG (Fig. 1d). Brighter areas correspond to higher counts of PLL-g-PEG-specific $\text{C}_4\text{H}_7\text{O}^+$ ($m/z = 71$, PEG), $\text{C}_5\text{H}_{10}\text{N}^+$ ($m/z = 84$, PLL) and $\text{C}_4\text{H}_9\text{O}_2^+$ ($m/z = 89$, PEG) fragments [22,56]. The maximum number of counts of these fragments is 46. While the pattern remains visible, indicating some selectivity, PLL-g-PEG appears to be present around the pattern as well as on the DDP-coated TiO_2 areas of the pattern. Scale bar: $10\ \mu\text{m}$. (e) A ToF-SIMS image of the sample after exposure to serum (Fig. 1e. See also Fig. 3a). Brighter areas correspond to higher counts of the protein (amino acid)-characteristic $\text{C}_4\text{H}_8\text{N}^+$ ($m/z = 70$; asparagine, proline) and $\text{C}_5\text{H}_{12}\text{N}^+$ ($m/z = 86$; leucine, isoleucine) intensities [57]. The maximum number of counts of these fragments is 29. The pattern is once again clearly visible, indicating selective adsorption of the protein to the DDP-coated, hydrophobic TiO_2 areas. Analysis of corresponding high mass resolution ToF-SIMS spectra proves that the intensity present in the background outside the pattern is due to the PLL-g-PEG-specific $\text{C}_4\text{H}_7\text{O}^+$ ($m/z = 71$; PEG), $\text{C}_5\text{H}_{10}\text{N}^+$ ($m/z = 84$; PLL) and $\text{C}_4\text{H}_9\text{O}_2^+$ ($m/z = 89$; PEG) fragments rather than corresponding fragments of the adsorbed protein (not shown). Fluorescence microscopy results (Fig. 3a and d), confirm the selectivity these patterns display with respect to protein adsorption. Scale bar: $10\ \mu\text{m}$.

When this oxide pattern is exposed to an aqueous solution of alkane phosphate ammonium salt, e.g., dodecyl phosphate (DDP), an organized self-assembled

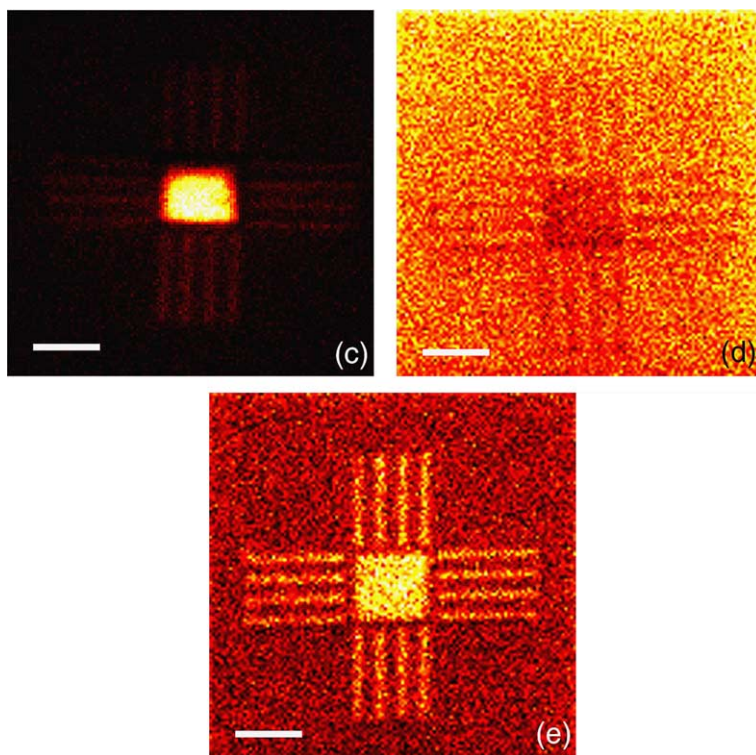


Fig. 2 (continued)

monolayer (SAM) is formed on TiO_2 (Fig. 1c) [23,24] very much like SAMs that are formed by alkanethiolates on gold. There is no interaction between DDP and SiO_2 and potential residual DDP on the SiO_2 surface is completely removed by rinsing with water. ToF-SIMS imaging confirms that the grooves and the square regions of the pattern are uniquely coated with DDP (Fig. 2c). Subsequent immersion in a buffered solution of poly(L-lysine)-*g*-poly(ethylene glycol), PLL-*g*-PEG, [25,26] the properties of which as a non-adhesive coating for negatively charged metal oxide surfaces are well-documented in the literature [27–29], results in adsorption of this polycationic graft co-polymer on the bare SiO_2 areas rendering them resistant to protein adsorption by virtue of the presentation of the non-ionic poly(ethylene glycol) domains of the graft co-polymer (Fig. 1d). DDP-coated areas are also covered with PLL-*g*-PEG (albeit to a lesser extent, Fig. 2d), presumably due to hydrophobic interactions, but upon exposure to a protein solution of choice, the adsorbing proteins readily replace residual PLL-*g*-PEG that is weakly adsorbed to these regions [22]. Therefore the TiO_2 regions modified with the methyl-terminated (and therefore hydrophobic) DDP are exclusively coated with the adsorbed proteins (Figs. 1e and 2e). This outstanding selectivity with respect to protein adsorption has been reported previously for patterns of other sizes [22,30], and is further confirmed in the

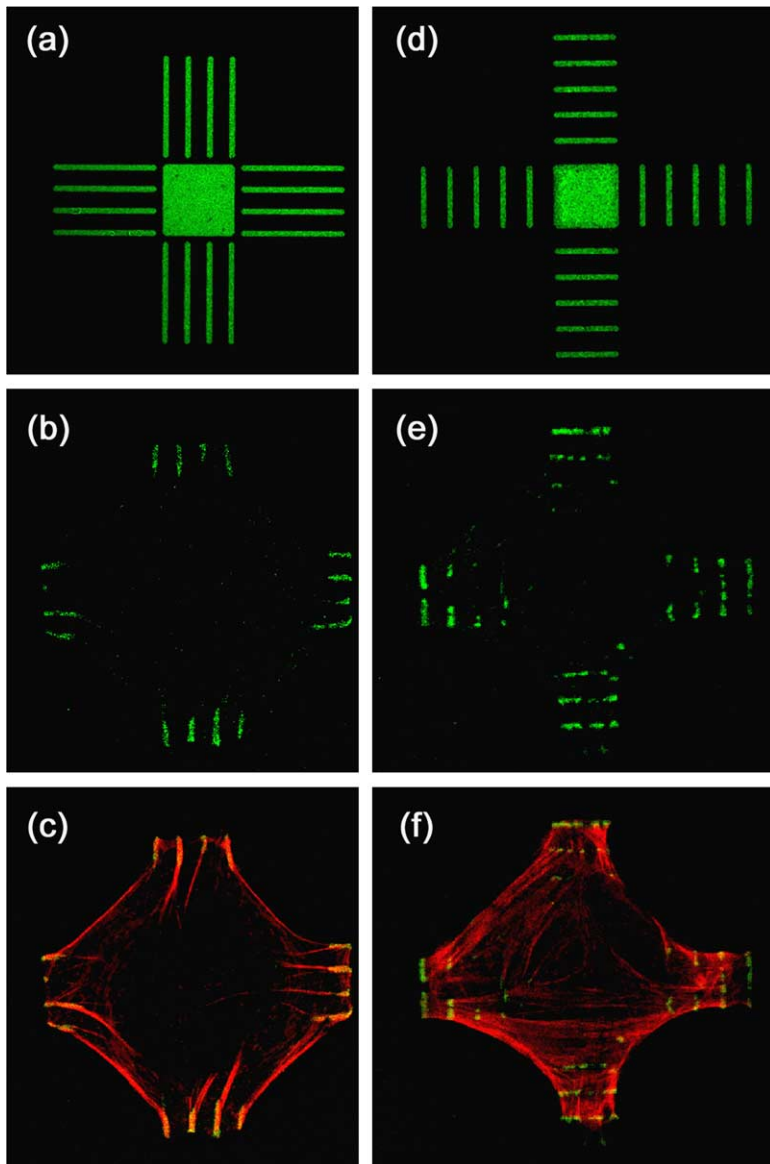


Fig. 3. Cell behaviour on subcellular SMAP patterns. (a) and (d) Fluorescence microscopy images of fibronectin, a prominent cell adhesion-promoting protein present in serum, on SMAP patterns. Samples were exposed to DMEM containing 10% FBS during 2 h at room temperature, rinsed with pure DMEM, and visualised by immuno-fluorescent staining. Fibronectin and other serum proteins adsorbed selectively to the DDP-domains of the SMAP surface. (b) and (e) Focal contacts, visualised by immunostaining for vinculin, a protein present on the cytoplasmatic side of focal contacts, are located exclusively on the adhesive fibronectin lines and in the peripheral regions of the cell. (c) and (f) Stress fibres are visualised by immunostaining for f-actin. Their anchoring points co-localise with focal contact sites and are thus also subjected to the constraints of the patterns.

case of the patterns used in this study by exposing them to serum-containing cell culture media, immunostaining for fibronectin, and examining them by fluorescence microscopy (Fig. 3a and d).

The means by which material contrast is created in the pre-patterning step (Fig. 1a and b) is irrelevant as far as surface modification procedures used in the subsequent steps (Fig. 1c–e) are concerned and as long as the DDP-PLL-*g*-PEG chemistry can be applied. In this and previous work, SMAP has been shown to be compatible with techniques such as standard optical lithography [22] and novel colloidal lithography [30]. Other, less conventional, techniques such as focused ion-beam [31], interference contrast [13,32,33], dip-pen [34], and electron beam [35] lithography, can also be used. This de-coupling of the pre-patterning (Fig. 1a and b) and surface modification (Fig. 1c–e) steps, without the use of stamps or other intermediates, is one of the keys to the flexibility of SMAP. The other key is the exploitation of spontaneous molecular assembly processes, entirely from aqueous solutions, resulting in simplicity of the approach that allows delicate surface chemistries to be incorporated into its protocols.

Substrates patterned with the SMAP technology can effectively serve as a generic platform in studies of mechanisms of cell adhesion at the cellular and sub-cellular level. An example is shown in Fig. 3, where human dermal fibroblasts were incubated in serum-containing media on the patterned surfaces and attached to two types of single cell-sized patterns. Both patterns exhibited the same overall shape (“Swiss cross”), but the arms of the crosses consisted of longitudinal bars of 15 μm length and 1 μm width in one case (Fig. 3a–c; the pattern described in Fig. 2) and of transverse bars of the same width but 10 μm length in the other case (Fig. 3d–f). The surface characterisation performed on the latter pattern yielded identical results to those shown in Fig. 2 (data not shown). Upon exposure to serum-containing cell-culture media, the adhesive regions of both patterns became coated with serum proteins (Fig. 3a and d). Proteins like fibronectin and vitronectin contained in the extracellular matrix (ECM) in vivo or cell culture media in vitro are essential factors mediating cell attachment to surfaces of artificial materials. The attachment of cells to surfaces coated with these extracellular matrix (ECM) molecules is mediated by a family of transmembrane proteins called integrins [36], which serve as linkers between the ECM and the elements of the cytoskeleton (actin fibres) inside the cell [37,38]. The linkage involves a number of other proteins, including vinculin, immunostaining for which was used to identify focal contacts, i.e., clusters that integrins and linkage proteins form upon binding to the ECM molecules.

Vinculin staining (Fig. 3b and e) demonstrates that cells attached to and formed focal contacts only on the regions of the patterns on which adhesion proteins, such as fibronectin, were present. No interaction with the protein-repulsive regions was observed at the time point of sample fixation (20 h). Actin stress fibres leading to these sites were identified by staining with fluorescent phalloidin (Fig. 3c and f). Interestingly, on the crosses with transverse bars, the stress fibres were coupled to the focal contacts perpendicular to the long axis of the bar, in spite of the restricted extent of the focal contacts in that direction (Fig. 3f). This observation is especially striking in view of previous studies in which a correlation between the focal contact extension

and direction of the force applied to the contact was found [39], and in view of studies involving surfaces with grooved morphology, where cells were found to align parallel to the grooves [40–42]. It appears that the orientation of the substrate features, focal contacts, and actin fibres do not necessarily correlate (Fig. 3c and f).

In addition to serving as transmembrane linkers between the ECM proteins and cytoskeleton elements, integrins perform vital signalling functions in the cell [43]. Variations in the expression and surface distribution of integrins correlate with the propensity of cells to migrate, incorporate into foreign tissues (in the case of metastatic cancer cells), and undergo apoptosis [44,45]. On the other hand, effects of the feature geometry of the surface pattern on cell polarity have been reported [14,15], and feature size was shown to have an effect on cell differentiation and activation of apoptotic pathways [14,16]. Yet, the understanding of the molecular links between these phenomena is largely missing. The need to extend the feature size of the patterns to the sub- μm range in order to understand how the geometrical and topographical signals of one focal adhesion are converted into specific cell functions and what effects *sub-cellular* variations in surface morphology have on cell phenotype is highlighted by the observation that at a length scale of 1 μm the focal contact morphology is not yet limited to a scale at which it affects the local mechanical coupling of adhesion site and stress fibres (Fig. 3f). It has already been demonstrated that SMAP is capable of handling nm-scale patterns prepared with a suitable pre-patterning technique [30] and cell studies on such nm-sized features are in progress.

In addition to pure adhesion contrast that is obtained with SMAP, patterns produced by this method also exhibit a small topographic contrast, i.e., a step between the protein-adhesive and protein-repulsive regions. The depth of the patterns used in this study was 15–25 nm, which is in a regime where chemical cues prevail over topographical ones [46,47] and topography alone is not expected to have an effect on cell behaviour [48,49].

The SMAP patterning approach presented here is based on the selective adsorption of methyl-terminated alkane phosphates discriminating between different oxides. Numerous variations of this selective adsorption process can be envisioned and are under investigation in our laboratories with the common characteristic that the desired geometries of the patterns are created in oxides on the substrates of choice. Subsequent translation into a (bio)chemically relevant contrast is achieved by exposure to a solution of the molecules to be adsorbed or grafted, such as ω -functionalized alkane phosphates [50] and PEGs or other functional polymers exposing either chemically or biochemically active groups such as recognition peptides [51,52] or antibodies [53].

SMAP has been successfully applied to create protein patterns with dimensions ranging from several hundreds of micrometers down to tens of nanometers [22,30]. Its limitations lie in the surface structuring methods available as well as the molecular sizes of the adsorbing species but not in the surface modification process itself. Given the availability of adequate nanoscale pre-patterning techniques, SMAP is likely to allow the probing of biological function at the level of single biomolecules.

A particular attractive option of future SMAP applications is to combine this technique with topographical micro- or nanoscale structuring during the

pre-structuring process. By varying the thickness of the SiO₂ and TiO₂ coatings (Fig. 1a) as well as etching times (Fig. 1b), structures with controlled depths of grooves, pits, or pillars [30] can be produced. When the material contrast is converted into a biological contrast on these surfaces, the proteins will be localised either at the bottom, the bottom and the walls, or at the top and walls of the grooves, pits, or pillars, as desired. Such nanostructured surfaces combining designed topography and biochemical contrast at nanometer length scales are attractive platforms for studying isolated single biomolecules and the effect of their placement in the third dimension [54] (i.e. at the bottom of a nanohole with non-interactive walls or at the top of a nanopillar) on the behaviour of cells.

In conclusion, SMAP is presented as a generic platform for the biotechnology field to produce biologically relevant 2D patterns as well as 3D surface structures that present biological functionalities at geometrically well-defined interfacial architectures. The strength of this novel technique lies in the exploitation of the advantages from combining a top-down approach (e.g. lithography, compatible with large scale, state-of-the-art fabrication) with a bottom-up approach that benefits from the gentle and cost-effective self-organization of chemical and biological moieties from aqueous solutions at room temperature.

2. Experimental

To facilitate the application of the SMAP technique by the interested readers, we end this Progress Highlight article with a set of concrete specifications for the methodology used in the experiments described.

2.1. Substrate preparation

Whole, 4-inch silicon wafers (Wafernet GmbH, Munich, Germany) were coated with 50 nm of TiO₂, and then with 12 nm of SiO₂, by reactive sputtering using a Leybold dc-magnetron Z600 sputtering plant. This process results in the tri-layer structure shown in Fig. 1a. The thickness of the individual layers was measured by spectroscopic ellipsometry (M-2000, Woollam, Lincoln, NE, USA). The coating procedure and the properties of the coatings have been reported previously [55].

2.2. Pre-patterning: creating material contrast

Dust particles were removed from coated wafers with a stream of nitrogen, before the wafers were heated to 115–120 °C to remove adsorbed contaminants, cooled, and spin-coated with Shipley S1818-SP16 photoresist (Micro Resist Technology, Berlin, Germany). The photoresist was diluted with microposit EC-solvent in a ratio 1:1 in order to lower the resist thickness to 0.5 μm (rotation speed 4000 rpm). Excess solvent was removed by heating the coated wafer to 115 °C for 120 s, which also hardened the resist.

The desired patterns were formed in the resist by exposing it in an Electronic Vision A16-2 mask aligner (EV Group, Schaerding, Austria) for 6 s through a mask specifically designed for the making of these patterns (Cromium Mask, Photonics SA, Neuchatel, Switzerland). Exposed wafers were developed for 20–30 s with a Shipley Microposit 351 developer (Micro Resist Technology, Berlin, Germany) diluted 1:5 with ultrapure water. Wafers were rinsed with ultrapure water and dried. Feature height was checked with a Tencor Alpha Step 200 height stepper (Brumley South Inc, Mooresville, NC, USA) to determine the resist thickness and with an optical microscope to ensure pattern quality.

Wafers with the features of the structured resist on them were transferred to a Surface Technology Systems STS T20 dry etching plant (Surface Science and Technology, Ulm, Germany), where the top SiO₂ layer was etched with a mixture of 6 sccm CF₄, 25 sccm CHF₃, O₂, at 50 mtorr, 300 K and 175 W. The corresponding average etch rate was determined to be typically 0.17 nm/s using a combination of AFM and ellipsometry. Etch times were chosen to guarantee that this process exposed the underlying TiO₂ in areas not covered by resist.

The resist was removed by first exposing it to oxygen plasma (in the dry etching plant) for 40 s and then to resist remover solution (Micro Resist Technology GmbH, Berlin, Germany) for 10 min at 60 °C. Residual contamination was removed by rinsing the wafers with acetone and ultrapure water. Clean wafers were cut into 1 × 1 cm² chips with a wafer saw (Kulike and Soffa, Israel), which were used in the subsequent surface modification steps. After lithography and etching, the substrates exhibited patterns such as those shown in Figs. 1b and 2a and b.

2.3. Surface modification: creating adhesion contrast

The chips bearing material contrast were cleaned by sonicating in 2-propanol for 5 min, blown dry with a stream of nitrogen, and treated with oxygen plasma in a plasma cleaner (Harrick Scientific Corporation, Ossining, NY, USA) for 3 min. Clean samples were exposed to an aqueous 0.5 mM solution of dodecyl phosphate ammonium salt (DDP) for at least 24 h and rinsed with high purity water. This step resulted in the formation of a DDP SAM on the TiO₂ regions of the patterns (Figs. 1c and 2c). Bare silicon dioxide regions were covered with poly(L-lysine)-graft-poly(ethylene glycol) (PLL-g-PEG) by exposing the samples to 1 mg/ml polymer dissolved in Hepes Z1 buffer (10 mM 4(2-hydroxyethyl)piperazine-1-ethanesulfonic acid, adjusted to pH 7.4) for 15 min (Figs. 1d and 2d). Excess PLL-g-PEG was removed by washing the substrates with the HEPES Z1 buffer. After the last step, the patterns are ready for protein adsorption and cell adhesion experiments.

2.4. Surface characterisation

The pre-patterns exhibiting material contrast (Figs. 1b and 2b) and the patterns with the developed chemical contrast (Figs. 1d and 2d) were characterised by a combination of X-ray photoelectron spectroscopy (XPS), time-of-flight secondary ion mass spectrometry (ToF-SIMS), atomic force microscopy, and fluorescence

microscopy. The procedure and results of XPS characterisation will not be described here as they are essentially identical to the previously published accounts [22,30].

2.4.1. Fluorescence microscopy (FM)

The adhesion contrast of the patterned surfaces (Figs. 1d and 2d) was evaluated by incubating the chips with a Dulbecco's Modified Eagle Medium (DMEM) supplemented with 10% foetal bovine serum (FBS) for 2 h at room temperature and rinsing with pure DMEM. Fibronectin, adsorbed to the DDP-covered hydrophobic areas of the pattern (Figs. 1e and 2e), was visualised by immunostaining with rabbit anti-fibronectin antibody (Dako, Glostrup, Denmark) and followed by Oregon-Green488-labelled goat anti-rabbit IgG (Molecular Probes, Eugene, OR, USA). The samples were rinsed with phosphate-buffered saline (PBS), mounted in mounting media (Immu-Mount, Shandon, Pittsburgh, PA), and observed in the Zeiss Axiovert 100M fluorescence microscope (Zeiss, Jena, Germany) with a 63×/1.25 NA Plan-Neofluar or 100×/1.4 NA Plan-Apochromat oil-immersion objective, using the LSM 510 confocal scanning module.

2.4.2. Time-of-flight secondary ion mass spectrometry (ToF-SIMS)

ToF-SIMS images of positively and negatively charged secondary ions were acquired using an ION-TOF TOF-SIMS IV instrument equipped with a liquid metal ion gun able to emit Au_n^+ cluster ions, a mass analyzer of the reflectron type and a low energy electron flood gun for charge compensation. For the presented results Au_1^+ bombardment was used. Most data were taken at nominal mass resolution of approximately 5000 and a lateral resolution of less than 400 nm (so-called burst alignment mode). In order to verify peak assignments, additional images were taken at high mass resolution (higher mass resolution than in burst alignment mode) and a focus size of 3 μm (bunched mode). The primary ion dose density did not exceed 5×10^{13} ions/ cm^2 .

2.4.3. Atomic force microscopy (AFM)

Samples exhibiting material contrast (Fig. 1b) were mounted on PTFE-covered metal disks and observed in a Nanoscope IIIa MultiMode AFM (Veeco Metrology, Inc., Santa Barbara, CA, USA) equipped with a "J" (120 μm) scanner. Observations were performed in fluid, in contact mode. O-rings were not used to avoid artefacts.

2.4.4. Cell experiments

Human foreskin fibroblasts (HFF) were kept in culture under standard cell-culture conditions. For the experiments they were trypsinized and resuspended in DMEM (Gibco, Coon Rapids, MN, USA) supplemented with 10% FBS and 1% antibiotic/antimycotic solution (Gibco, Coon Rapids, MN, USA) and seeded on single SMAP substrates placed in 24-well plates at 10,000–15,000 cells per well. Samples were incubated for 20 h at 37° under a 5% CO_2 atmosphere, after which time cells were fixed with 4% paraformaldehyde in PBS for 15 min at room temperature, permeabilized with 0.1% Triton X-100 in PBS for 5 min and immunostained for vinculin with a primary mouse anti-vinculin/secondary AF-488-labelled chicken anti-mouse

antibody (Molecular Probes, Eugene, OR, USA) combination and for actin with phalloidin-AF594 (Molecular Probes, Eugene, OR, USA). The samples were then mounted in mounting media (Immu-Mount, Shandon, Pittsburgh, PA, USA) and observed in a fluorescence microscope (see Section 2.4.1 above). All reagents were purchased from Sigma-Aldrich except where mentioned otherwise.

Acknowledgments

We would like to thank Prof. H. Baltes, Dr. A. Hierlemann, and D. Scheiwiler (Physical Electronics Laboratory, ETHZ) for access and introduction to their clean room facilities, Michael Horisberger (Paul Scherrer Institute, PSI, Villigen, Switzerland) for the sputter coating of the substrates and Dr. B. Hagenhoff and E. Tallarek (TASCON GmbH, Germany) for the ToF-SIMS measurements and Dr. J. Vörös for stimulating discussions. This work is financially supported by the TOP NANO 21 Program of the ETH-Council (project KTI 4597.1).

References

- [1] P. Peluso, D.S. Wilson, D. Do, H. Tran, M. Venkatasubbaiah, D. Quincy, B. Heidecker, K. Poindexter, N. Tolani, M. Phelan, K. Witte, L.S. Jung, P. Wagner, S. Nock, Optimizing antibody immobilization strategies for the construction of protein microarrays, *Anal. Biochem.* 312 (2003) 113–124.
- [2] A.Q. Emili, G. Cagney, Large-scale functional analysis using peptide or protein arrays, *Nat. Biotechnol.* 18 (2000) 393–397.
- [3] K.E. Vrana, W.M. Freeman, M. Aschner, Use of microarray technologies in toxicology research, *Neurotoxicology* 24 (2003) 321–332.
- [4] T.H. Park, M.L. Shuler, Integration of cell culture and microfabrication technology, *Biotechnol. Progr.* 19 (2003) 243–253.
- [5] B.D. Boyan, C.H. Lohmann, D.D. Dean, V.L. Sylvia, D.L. Cochran, Z. Schwartz, Mechanisms involved in osteoblast response to implant surface morphology, *Ann. Rev. Mater. Res.* 31 (2001) 357–371.
- [6] B. Kasemo, Biological surface science, *Surf. Sci.* 500 (2002) 656–677.
- [7] H.G. Craighead, C.D. James, A.M.P. Turner, Chemical and topographical patterning for directed cell attachment, *Curr. Opin. Solid State Mater. Sci.* 5 (2001) 177–184.
- [8] S. Huang, D.E. Ingber, Shape-dependent control of cell growth, differentiation, and apoptosis: switching between attractors in cell regulatory networks, *Exp. Cell Res.* 261 (2000) 91–103.
- [9] G. Albrecht-Buehler, The angular distribution of directional changes of guided 3T3 cells, *J. Cell Biol.* 80 (1979) 53–60.
- [10] R. Singhvi, G. Stephanopoulos, D.I.C. Wang, Effects of substratum morphology on cell physiology, *Biotechnol. Bioeng.* 43 (1994) 764–771.
- [11] D.M. Brunette, B. Chehroudi, The effects of the surface topography of micromachined titanium substrata on cell behavior in vitro and in vivo, *J. Biomech. Eng.—T. Asme* 121 (1999) 49–57.
- [12] Y.N. Xia, G.M. Whitesides, Soft lithography, *Annu. Rev. Mater. Sci.* 28 (1998) 153–184.
- [13] G.M. Whitesides, E. Ostuni, S. Takayama, X.Y. Jiang, D.E. Ingber, Soft lithography in biology and biochemistry, *Annu. Rev. Biomed. Eng.* 3 (2001) 335–373.
- [14] K.K. Parker, A.L. Brock, C. Brangwynne, R.J. Mannix, N. Wang, E. Ostuni, N.A. Geisse, J.C. Adams, G.M. Whitesides, D.E. Ingber, Directional control of lamellipodia extension by constraining cell shape and orienting cell tractional forces, *Faseb. J.* 16 (2002) 1195–1204.

- [15] A. Brock, E. Chang, C.C. Ho, P. LeDuc, X.Y. Jiang, G.M. Whitesides, D.E. Ingber, Geometric determinants of directional cell motility revealed using microcontact printing, *Langmuir* 19 (2003) 1611–1617.
- [16] C.S. Chen, M. Mrksich, S. Huang, G.M. Whitesides, D.E. Ingber, Geometric control of cell life and death, *Science* 276 (1997) 1425–1428.
- [17] R.S. Kane, S. Takayama, E. Ostuni, D.E. Ingber, G.M. Whitesides, Patterning proteins and cells using soft lithography, *Biomaterials* 20 (1999) 2363–2376.
- [18] M.E. Hasenbein, T.T. Andersen, R. Bizios, Micropatterned surfaces modified with select peptides promote exclusive interactions with osteoblasts, *Biomaterials* 23 (2002) 3937–3942.
- [19] N.D. Gallant, J.R. Capadona, A.B. Frazier, D.M. Collard, A.J. Garcia, Micropatterned surfaces to engineer focal adhesions for analysis of cell adhesion strengthening, *Langmuir* 18 (2002) 5579–5584.
- [20] R. Singhvi, A. Kumar, G.P. Lopez, G.N. Stephanopoulos, D.I.C. Wang, G.M. Whitesides, D.E. Ingber, Engineering cell-shape and function, *Science* 264 (1994) 696–698.
- [21] K. Glasmastar, J. Gold, A.S. Andersson, D.S. Sutherland, B. Kasemo, Silicone transfer during microcontact printing, *Langmuir* 19 (2003) 5475–5483.
- [22] R. Michel, J.W. Lussi, G. Csucs, I. Reviakine, G. Danuser, B. Ketterer, J.A. Hubbell, M. Textor, N.D. Spencer, Selective molecular assembly patterning: a new approach to micro- and nanochemical patterning of surfaces for biological applications, *Langmuir* 18 (2002) 3281–3287.
- [23] R. Hofer, M. Textor, N.D. Spencer, Alkyl phosphate monolayers, self-assembled from aqueous solution onto metal oxide surfaces, *Langmuir* 17 (2001) 4014–4020.
- [24] M. Textor, L. Ruiz, R. Hofer, A. Rossi, K. Feldman, G. Hahner, N.D. Spencer, Structural chemistry of self-assembled monolayers of octadecylphosphoric acid on tantalum oxide surfaces, *Langmuir* 16 (2000) 3257–3271.
- [25] A.S. Sawhney, J.A. Hubbell, Poly(ethylene oxide)-*graft*-poly(L-lysine) copolymers to enhance the biocompatibility of poly(L-lysine)-alginate microcapsule membranes, *Biomaterials* 13 (1992) 863–870.
- [26] D.L. Elbert, J.A. Hubbell, Self-assembly and steric stabilization at heterogeneous, biological surfaces using adsorbing block copolymers, *Chem. Biol.* 5 (1998) 177–183.
- [27] G.L. Kenausis, J. Vörös, D.L. Elbert, N.P. Huang, R. Hofer, L. Ruiz-Taylor, M. Textor, J.A. Hubbell, N.D. Spencer, Poly(L-lysine)-*g*-poly(ethylene glycol) layers on metal oxide surfaces: Attachment mechanism and effects of polymer architecture on resistance to protein adsorption, *J. Phys. Chem. B* 104 (2000) 3298–3309.
- [28] N.P. Huang, R. Michel, J. Vörös, M. Textor, R. Hofer, A. Rossi, D.L. Elbert, J.A. Hubbell, N.D. Spencer, Poly(L-lysine)-*g*-poly(ethylene glycol) layers on metal oxide surfaces: Surface-analytical characterization and resistance to serum and fibrinogen adsorption, *Langmuir* 17 (2001) 489–498.
- [29] L.A. Ruiz-Taylor, T.L. Martin, F.G. Zaugg, K. Witte, P. Indermuhle, S. Nock, P. Wagner, Monolayers of derivatized poly(L-lysine)-grafted poly(ethylene glycol) on metal oxides as a class of biomolecular interfaces, *Proc. Nat. Acad. Sci. USA* 98 (2001) 852–857.
- [30] R. Michel, I. Reviakine, D. Sutherland, C. Fokas, G. Csucs, G. Danuser, N.D. Spencer, M. Textor, A novel approach to produce biologically relevant chemical patterns at the nanometer scale: selective molecular assembly patterning combined with colloidal lithography, *Langmuir* 18 (2002) 8580–8586.
- [31] J. Melngailis, A.A. Mondelli, I.L. Berry, R. Mohondro, A review of ion projection lithography, *J. Vac. Sci. Technol. B* 16 (1998) 927–957.
- [32] J.A. Rogers, K.E. Paul, R.J. Jackman, G.M. Whitesides, Using an elastomeric phase mask for sub-100 nm photolithography in the optical near field, *Appl. Phys. Lett.* 70 (1997) 2658–2660.
- [33] J.A. Rogers, K.E. Paul, R.J. Jackman, G.M. Whitesides, Generating similar to 90 nanometer features using near-field contact-mode photolithography with an elastomeric phase mask, *J. Vac. Sci. Technol. B* 16 (1998) 59–68.
- [34] R.D. Piner, J. Zhu, F. Xu, S.H. Hong, C.A. Mirkin, Dip-pen nanolithography, *Science* 283 (1999) 661–663.
- [35] Y. Chen, A. Pepin, Nanofabrication: conventional and nonconventional methods, *Electrophoresis* 22 (2001) 187–207.
- [36] R.O. Haynes, Integrins: a family of cell surface receptors, *Cell* 48 (1987) 549–554.
- [37] K. Burridge, M. Chrzanowska-Wodnicka, Focal adhesions, contractility, and signaling, *Annu. Rev. Cell Dev. Biol.* 12 (1996) 463–518.

- [38] B. Geiger, A. Bershadsky, R. Pankov, K.M. Yamada, Transmembrane extracellular matrix-cytoskeleton crosstalk, *Nat. Rev. Mol. Cell Biol.* 2 (2001) 793–805.
- [39] N.Q. Balaban, U.S. Schwarz, D. Riveline, P. Goichberg, G. Tzur, I. Sabanay, D. Mahalu, S. Safran, A. Bershadsky, L. Addadi, B. Geiger, Force and focal adhesion assembly: a close relationship studied using elastic micropatterned substrates, *Nat. Cell Biol.* 3 (2001) 466–472.
- [40] A. Curtis, C. Wilkinson, Topographical control of cells, *Biomaterials* 18 (1997) 1573–1583.
- [41] X.Y. Jiang, S. Takayama, X.P. Qian, E. Ostuni, H.K. Wu, N. Bowden, P. LeDuc, D.E. Ingber, G.M. Whitesides, Controlling mammalian cell spreading and cytoskeletal arrangement with conveniently fabricated continuous wavy features on poly(dimethylsiloxane), *Langmuir* 18 (2002) 3273–3280.
- [42] X.F. Walboomers, W. Monaghan, A.S.G. Curtis, J.A. Jansen, Attachment of fibroblasts on smooth and microgrooved polystyrene, *J. Biomed. Mater. Res.* 46 (1999) 212–220.
- [43] M.A. Schwartz, Integrin signaling revisited, *Trends Cell Biol.* 11 (2001) 466–470.
- [44] J.D. Hood, D.A. Cheresh, Role of integrins in cell invasion and migration, *Nat. Rev. Cancer* 2 (2002) 91.
- [45] R.G. Lebaron, K.A. Athanasiou, Extracellular matrix cell adhesion peptides: functional applications in orthopedic materials, *Tissue Eng.* 6 (2000) 85–103.
- [46] A.S.G. Curtis, C.D. Wilkinson, Reactions of cells to topography, *J. Biomater. Sci.—Polymer Ed.* 9 (1998) 1313–1329.
- [47] S. Britland, H. Morgan, B. WojciakStodart, M. Riehle, A. Curtis, C. Wilkinson, Synergistic and hierarchical adhesive and topographic guidance of BHK cells, *Exp. Cell Res.* 228 (1996) 313–325.
- [48] B. Wojciak-Stothard, A. Curtis, W. Monaghan, K. Macdonald, C. Wilkinson, Guidance and activation of murine macrophages by nanometric scale topography, *Exp. Cell Res.* 223 (1996) 426–435.
- [49] Control experiments were performed with homogeneously adhesive substrates (prepatterned oxide substrates without the SMAP treatment), which were found not to affect cell behaviour (data not shown). See M. Winkelmann, J. Gold, R. Hauert, B. Kasemo, N.D. Spencer, D.M. Brunette, M. Textor, Chemically patterned, metal oxide based surfaces produced by photolithographic techniques for studying protein- and cell-surface interactions I: Microfabrication and surface characterization, *Biomaterials* 7 (2002) 1133–1145.
- [50] S. Tosatti, R. Michel, M. Textor, N.D. Spencer, Self-assembled monolayers of dodecyl and hydroxy-dodecyl phosphates on both smooth and rough titanium and titanium oxide surfaces, *Langmuir* 18 (2002) 3537–3548.
- [51] S. VandeVondele, J. Vörös, J.A. Hubbell, RGD-Grafted poly(L-lysine)-graft-(polyethylene glycol) copolymers block non-specific protein adsorption while promoting cell adhesion, *Biotech. Bioeng.* 82 (2003) 784–790.
- [52] S. Tosatti, Z. Schwartz, C. Campbell, D.L. Cochran, S. VandeVondele, J.A. Hubbell, A. Denzer, J. Simpson, M. Wieland, C.H. Lohmann, M. Textor, B.D. Boyan, RGD-containing peptide GCRGYGRGDSPG reduces enhancement of osteoblast differentiation by poly(L-lysine)-graft-poly(ethylene glycol)-coated titanium surfaces, *J. Biomed. Mater. Res. A* 68A (2004) 458–472.
- [53] N.P. Huang, J. Vörös, S.M. De Paul, M. Textor, N.D. Spencer, Biotin-derivatized poly(L-lysine)-g-poly(ethylene glycol): A novel polymeric interface for bioaffinity sensing, *Langmuir* 18 (2002) 220–230.
- [54] B. Geiger, Cell biology—encounters in space, *Science* 294 (2001) 1661.
- [55] R. Kurrat, M. Textor, J.J. Ramsden, P. Boni, N.D. Spencer, Instrumental improvements in optical waveguide light mode spectroscopy for the study of biomolecule adsorption, *Rev. Sci. Instrum.* 68 (1997) 2172–2176.
- [56] S. Pasche, S.M. De Paul, J. Vörös, N.D. Spencer, M. Textor, Poly(L-Lysine)-graft-poly(ethylene glycol) assembled monolayers on niobium oxide surfaces: a quantitative study of the influence of polymer interfacial architecture on resistance to protein adsorption by ToF-SIMS and in situ OWLS, *Langmuir*, (2003) 9216–9225.
- [57] M.S. Wagner, S.L. McArthur, M.C. Shen, T.A. Horbett, D.G. Castner, Limits of detection for time of flight secondary ion mass spectrometry (ToF-SIMS) and X-ray photoelectron spectroscopy (XPS): detection of low amounts of adsorbed protein, *J. Biomater. Sci.—Polymer Ed.* 13 (2002) 407–428.